ScientificScholar®
Knowledge is power
Publisher of Scientific Journals

www.clinicalimagingscience.org

Journal of Clinical Imaging Science

Cardiopulmonary Imaging *Original Research*

A Pilot Study to Estimate the Impact of High Matrix Image Reconstruction on Chest Computed Tomography

Akitoshi Inoue[1], Tucker F. Johnson[1], Benjamin A. Voss[1], Yong S. Lee[1], Shuai Leng[1], Chi Wan Koo[1], Brian D. McCollough[1], Jayse M. Weaver[1], Hao Gong[1], Rickey E. Carter[2], Cynthia H. McCollough[1], Joel G. Fletcher[1]

[1]Departments of Radiology, [2]Clinical Trials and Biostatistics, Mayo Clinic, Rochester, Minnesota, United States.

***Corresponding author:**
Tucker F. Johnson,
Department of Radiology, Mayo Clinic, Rochester, Minnesota, United States.

tucker.f.johnson.md@gmail.com

Received : 20 July 2021
Accepted : 14 September 2021
Published : 30 September 2021

DOI
10.25259/JCIS_143_2021

Quick Response Code:

ABSTRACT

Objectives: The objectives of the study were to estimate the impact of high matrix image reconstruction on chest computed tomography (CT) compared to standard image reconstruction.

Material and Methods: This retrospective study included patients with interstitial or parenchymal lung disease, airway disease, and pulmonary nodules who underwent chest CT. Chest CT images were reconstructed using high matrix (1024 × 1024) or standard matrix (512 × 512), with all other parameters matched. Two radiologists, blinded to reconstruction technique, independently examined each lung, viewing image sets side by side and rating the conspicuity of imaging findings using a 5-point relative conspicuity scale. The presence of pulmonary nodules and confidence in classification of internal attenuation was also graded. Overall image quality and subjective noise/artifacts were assessed.

Results: Thirty-four patients with 68 lungs were evaluated. Relative conspicuity scores were significantly higher using high matrix image reconstruction for all imaging findings indicative of idiopathic lung fibrosis (peripheral airway visualization, interlobular septal thickening, intralobular reticular opacity, and end-stage fibrotic change; $P \leq 0.001$) along with emphysema, mosaic attenuation, and fourth order bronchi for both readers ($P \leq 0.001$). High matrix reconstruction did not improve confidence in the presence or classification of internal nodule attenuation for either reader. Overall image quality was increased but not subjective noise/artifacts with high matrix image reconstruction for both readers ($P < 0.001$).

Conclusion: High matrix image reconstruction significantly improves the conspicuity of imaging findings reflecting interstitial lung disease and may be useful for diagnosis or treatment response assessment.

Keywords: Image reconstruction, Interstitial lung disease, Idiopathic pulmonary fibrosis, Airway disease, Pulmonary nodule

INTRODUCTION

High-resolution computed tomography (HRCT) has historically improved visualization of the lung anatomy, including the peripheral bronchi, pulmonary vessels, and interlobular septa.[1] Numerous radiologic-pathologic correlational studies have been performed using HRCT for interstitial lung diseases,[2] airway disease,[3] lymphangitic diseases,[4] and for pulmonary nodules,[5] demonstrating HRCT's ability to display details seen at subsequent pulmonary histopathology. At present, HRCT plays an important role in diagnosing lung diseases, including, classifying and monitoring interstitial lung diseases[6] as well as pulmonary nodules.[7]

While newer computed tomography (CT) systems substantially lower radiation dose and implement faster table speeds, techniques to improve spatial resolution have lagged. The development of an ultra-HRCT system in 2011 allowed detector element sizes of 0.25 × 0.25 mm and spatial resolution of 120 μm.[8] Current ultra-HRCT can provide images with matrix sizes of 1024 × 1024 or 2048 × 2048 compared to the standard matrix size of 512 × 512, improving image quality for pulmonary nodules *in vivo*[8] and imaging findings of diffuse lung disease in cadaveric lungs with diffuse lung diseases.[9,10]

At present, ultra-HRCT systems are not widely available and nearly all chest CT images are created using a standard image reconstruction matrix of 512 × 512. Recently, Bartlett *et al*. have shown that high matrix image reconstruction using a 1024 × 1024 matrix with a photon-counting CT system improved the detection of higher-order bronchi.[11] Based on these findings, we hypothesized that high matrix image reconstruction with 1024 × 1024 matrix using a conventional CT system with an energy-integrating detector could improve the conspicuity of normal anatomy and abnormal findings of various lung diseases, including interstitial lung diseases, airway diseases, and pulmonary nodules. The purpose of this study is, therefore, to estimate the impact of high matrix image reconstruction on chest CT compared to our current practice of standard image reconstruction for evaluation of lung disease.

MATERIAL AND METHODS

Patients

This retrospective study was approved by our institutional review board (IRB number: 19-000961). Participating patients consented to the retrospective use of medical records and materials for research purposes. A chest radiologist (T.F.J. with 7 years of chest imaging experience) searched for adult patients (age ≥18) with any lung pathologies displayed on a clinical HRCT scan performed on a 192-slice CT scanner (Definition Force; Siemens Healthineers, Forchheim, Germany) and who had archived projection CT data as part of a clinical registry between January 2017 and December 2018.

CT protocol

CT examinations were performed using a 192-slice CT scanner (Definition Force, Siemens Healthineers) with a routine chest protocol without contrast or pulmonary embolism CT protocol with contrast. All images were reconstructed at both 512 × 512 (standard image reconstruction) and 1024 ×1024 matrix sizes (high matrix image reconstruction) using software on the scanner (Precision Matrix; Siemens Healthineers). Scanning and reconstruction parameters are summarized in Table 1.

Image analysis

During reading sessions, a co-author (B.D.M.) displayed the paired images (standard image reconstruction and high matrix image reconstruction) side by side in a random fashion (i.e. high matrix image reconstruction on the left or right monitor) on two diagnostic quality monitors using a workstation (syngo.via; Siemens Healthineers). In each reading session, images were identically enlarged on the two monitors to display either the right or left lung using a predetermined randomization scheme (i.e. lung and reconstruction matrix assigned to the left and right monitor for each patient), with each patient's images shown only once per session. Two board-certificated radiologists (T.F.J and A.I with 7 and 6 years of chest imaging experience, respectively), who were blinded to clinical history, histopathological diagnosis, and image acquisition and reconstruction parameters, were asked to compare the left monitor to the right monitor. With this design, each lung was compared to itself with the only difference being the reconstruction matrix. Consequently, the readers had 68 image sets from 34 patients in the two reading sessions. The lung window setting was used for evaluation.

Image analysis began with readers panning up and down through images on both monitors to determine the presence of (1) peripheral airway visualization, (2) mosaic attenuation, (3) emphysema, (4) interlobular septal thickening, (5) intralobular reticular opacity, (6) bronchial wall thickening, and (7) end-stage fibrotic change, including traction bronchiectasis and honeycombing using a 5-point Likert scale (0) absent; (1) likely absent; (2) uncertain; (3) likely present; and (4) present. If a finding was rated as being present on at least one monitor, a score of three was assigned to at least one of the two sets of images.

Once a finding was identified as being present, readers evaluated the relative conspicuity of the abnormal imaging finding on each monitor using a standard grading system, comparing the images on the left monitor to images on the right monitor.[11] Readers were instructed to examine the abnormality on the right monitor, then examine the imaging finding on the left monitor and rate the conspicuity of the images on the left monitor using a 5-point relative conspicuity scale (-2, definitely worse, probable decreased ability to detect abnormalities; -1, definitely worse, unclear effect on potential diagnosis; 0, about the same or unclear benefit/decrement; +1, definitely better, unclear effect on potential diagnosis; +2, definitely better, probable increased ability to detect the finding).[11] The conspicuity of 3rd and 4th order bronchi was also specifically evaluated for all cases using the same 5-point relative conspicuity scale.

Subsequently, each radiologist reader selected up to four pulmonary nodules for image evaluation in patient scans where nodules were present. If there were more than four

Table 1: Summary of CT acquisition and reconstruction parameters.

Parameter	Chest Routine Protocol	Pulmonary Embolism Protocol
Scan type	Spiral	Spiral (Flash mode)
Rotation Time (s)	0.25	0.25
Collimation	192×0.6 (with z flying focal spot)	192×0.6 (with z flying focal spot)
Pitch	1.2	3
kVp	120	120
CareDose 4D	ON	ON
Quality Reference mAs*	80	180
CTDIvol (mGy)‡	5.35	7.61
Reconstruction		
Iterative Reconstruction Algorithm/Strength	ADMIRE/2	ADMIRE/2
Kernel	Bv49	Bv49
Slice Thickness (mm)	1.5	1.5
Slice Increment (mm)	1.0	1.0
Field of View	Patient size	Patient size

*Quality reference mAs is the product of tube current (mA) and rotation time (s) and is the effective mAs for a reference sized patient (70 kg) when CareDose 4D (the automatic exposure control technique used on Siemens scanners) is turned on. ‡: CTDIvol: volume CT dose index. The specific value of CTDIvol for each patient varies as CareDose 4D adjusts tube current, and consequently CTDIvol, according to patient size. Values provided here are for the reference sized patient (70 kg). Note that PE protocol may run into tube power limit at the high pitch value of 3, CT: Computed tomography

pulmonary nodules, the radiologists were asked to prioritize nodules for selection first by attenuation (1 – ground-glass attenuation and 2 – part solid nodules) and then by size (i.e. nodules with diameters between 3 mm and 7 mm). For each nodule, the likelihood that a nodule was present on each image type was rated (0–100 score) and then the nodule's internal attenuation was characterized (ground-glass and part-solid, solid). Subsequently, a score reflecting confidence in correctly classifying internal attenuation was given (0–100 score).

Finally, the radiologists rated overall image quality for the image set on each monitor, using a 3-point Likert scale (1 = poor image quality; 2 = fair image quality; and 3 = excellent image quality), in addition to grading subjective visual noise or artifact (1 = strong presence of noise or artifact; 2 = moderate presence; and 3 = absence to slight presence).

Statistical analysis

All CT images were examined by both readers and were randomly assigned over the course of two reading sessions. The analysis assumed no order effect in the data analysis, and statistics were computed by reader as well as a composite index, which averaged reader responses.

To test for systematic differences in ratings by reader as well as summarize the degree to which, if any, the readers agreed on the ratings, Krippendorff's alpha, and the generalized test of symmetry (i.e. an extension of McNemar's test to tables larger than 2 × 2) were constructed. Krippendorff's alpha is a generalized measure of agreement that allows for missing data (e.g. when one reader identified an abnormality as being present and the other rated it as being absent). For this paper, the alpha value is interpretable the same as the more commonly reported kappa and was categorized as none (<0), slight (0–0.20), fair (0.21–0.40), moderate (0.41–0.60), and substantial (0.61–0.80). Rejection of the null hypothesis in the symmetry test suggested differential perceptions by reader, potentially in terms of the quantification of the relative conspicuity by reader. Monte Carlo approximation of the exact multinomial test was used to produce the *P*-value for the test of symmetry.

A relative conspicuity score was used to reflect the differential ability of the two reconstructions to display each imaging finding and used by the readers in comparing images on the left monitor compared to images on the right monitor. For purposes of analysis, the reader data were converted, as appropriate, to represent the conspicuity of findings on the high matrix images in comparison to the routine images. Consequently, this scale, which ranged from -2 to + 2, had anchors of -2 indicating high matrix image reconstruction was much worse than routine standard image reconstruction, and + 2 indicating high matrix image reconstruction was much better, with 0 being non-differential. The Wilcoxon signed-rank test was used to test the hypothesis that the perceived performance was not different between the two reconstruction approaches stratified by reader. In addition, the mean conspicuity rating (along with 95% confidence intervals) for each imaging finding for each reader for each imaging finding was calculated.

Likert scales for the presence and confidence of classification of pulmonary nodules, and image quality and subjective noise and artifact were compared between two reconstructions using Wilcoxon signed-rank test.

For statistical tests, *P*-value of <0.05 was considered to indicate a statistically significant difference. Analyses were conducted by statistical software R version 3.6.2.

RESULTS

Patients

During the catchment period 243 patients had chest CT scans with archived projection data, with 39 having lung pathologies that qualified them for study inclusion. Five of the 39 patients were excluded because of a lack of permission to use health information for research purposes. Therefore, our cohort consisted of 34 patients (average age 64.7 ± 12.3 year old, M: F = 24:10) who had including interstitial lung disease (n = 12), sarcoidosis (n = 4), emphysema (n = 4), pneumonia (n = 4), bronchitis (n = 3), bronchial asthma (n = 1), amyloidosis (n = 1), graft-versus host disease (n = 1), or/and pulmonary nodules (n = 4). The field of view is determined by the patient size at our institution and Table 2 shows the estimated pixel sizes for patient images in our cohort, which ranged from 0.664–0.898 mm for routine reconstruction and 0.332–0.449 mm for high matrix reconstruction.

Presence of imaging findings

The majority of patients had peripheral airways that could be seen on routine or high matrix chest CT images, with other imaging findings seen in about one-third of the lungs examined. Reader agreement for the presence of mosaic attenuation (α = 0.444), emphysema (α = 0.584), and intralobular reticular opacity (α = 0.466) was moderate. Inter-observer agreement for interlobular septal thickening (α = 0.349) and end-stage fibrotic change (α=0.335) was fair, and agreement for bronchial wall thickening (α = 0.014) and peripheral airway visualization (α = –0.206) were slight and none, respectively.

Table 2: Estimated pixel size for patient images displayed using standard image reconstruction and high matrix image reconstruction.

Field of view (mm)	Number of patients	Estimated pixel size in standard image reconstruction (mm)	Estimated pixel sizes in high matrix image reconstruction (mm)
340	7	0.664	0.332
350	1	0.684	0.342
360	1	0.703	0.352
380	9	0.742	0.371
400	6	0.781	0.391
420	7	0.820	0.410
440	2	0.859	0.430
460	1	0.898	0.449

Conspicuity of imaging findings

Table 3 summarizes the relative conspicuity scores for each of the imaging findings on high matrix chest CT images relative to routine matrix, with scores of zero indicating relative equivalence. For conspicuity of 4th order bronchi, the score of high matrix image reconstruction was higher than that of routine standard image reconstruction for both readers (P < 0.001) [Figure 1].

For all tested imaging findings suggestive of idiopathic pulmonary fibrosis, including peripheral airway visualization, interlobular septal thickening, intralobular reticular opacity, and end-stage fibrotic change such as traction bronchiectasis and honeycombing, the scores for high matrix image reconstruction images were significantly higher than those of standard image reconstruction for both readers ($P \leq 0.001$) [Figures 2 and 3]. For mosaic attenuation and emphysema, high matrix image reconstruction showed higher scores than those of routine standard image matrix ($P \leq 0.001$) [Figure 4]. For bronchial wall thickening, there was not a significant difference between reconstructions for one reader (P = 0.072), although the score was higher than that of standard image reconstruction. Figure 5 shows the mean conspicuity scores for each imaging finding for each reader. For all imaging findings except for visualization of 3rd order bronchi, the lower end of the 95% confidence interval for the relative conspicuity score exceeded zero, with zero indicating no difference in ability of the reconstruction to display the imaging finding.

Lung nodules

In assessing lung nodules, reader 1 found 157 nodules in 59 lungs (72 solid, 34 part-solid, and 51 ground-glass nodules using standard image reconstruction), with the reader reclassifying one solid nodule and one ground-glass nodule as part-solid nodules using high matrix image reconstruction. Reader 2 found 130 nodules in 49 lungs (68 solid nodules, 6 part-solid nodules, and 56 ground-glass nodules using standard image reconstruction), with reader 2 reclassifying one ground-glass nodule as a solid nodule with high matrix image reconstruction. Table 4 shows the likelihood ratings for pulmonary nodule presence and confidence ratings for correct classification of internal attenuation characteristics. Regarding nodule presence, solid and part-solid nodules had similar likelihood ratings, with high matrix image reconstruction demonstrating a slightly higher likelihood of ground-glass nodules for one reader (P < 0.001). For confidence in correctly classifying internal attenuation characteristics as solid, part-solid or ground-glass, high matrix reconstruction significantly increased confidence for all types of nodules for one reader

Table 3: Mean relative conspicuity scores (SD) for the conspicuity of each imaging finding as visualized using high matrix image reconstruction images (1024×1024) compared to standard image reconstruction (512×512). A score of 0 indicated the structure or abnormality was seen equivalently between reconstructions. (Other scores: -2, high matrix image reconstruction definitely worse, probable decreased ability to see abnormalities; -1, high matrix image reconstruction definitely worse, unclear effect on potential diagnosis; +1, high matrix image reconstruction definitely better, unclear effect on potential diagnosis; +2, high matrix image reconstruction definitely better, probable increased ability to see abnormalities).

	Reader 1	*P*-value	Reader 2	*P*-value
Normal anatomy				
3rd brohchi	0 (0)	NA	0.68 (0.50)	<0.001*
4th bronchi	0.94 (0.54)	<0.001*	1.103 (0.49)	<0.001*
Abnormal findings				
Peripheral airway visualization	1.35 (0.77)	<0.001*	0.91 (0.75)	<0.001*
Mosaic attenuation	0.71 (0.81)	0.001*	1.42 (0.58)	<0.001*
Emphysema	1.16 (0.55)	<0.001*	1.42 (0.77)	<0.001*
Interlobular septal thickening	0.61 (0.50)	0.001*	0.92 (0.28)	<0.001*
Intralobular reticular opacity	1.47 (0.93)	<0.001*	0.90 (0.40)	<0.001*
Bronchial wall thickening	0.76 (0.61)	<0.001*	0.57 (0.54)	0.072
End stage fibrotic change	1.18 (0.95)	<0.001*	0.95 (0.61)	<0.001*

Wilcoxon-signed rank test,*: $P<0.05$

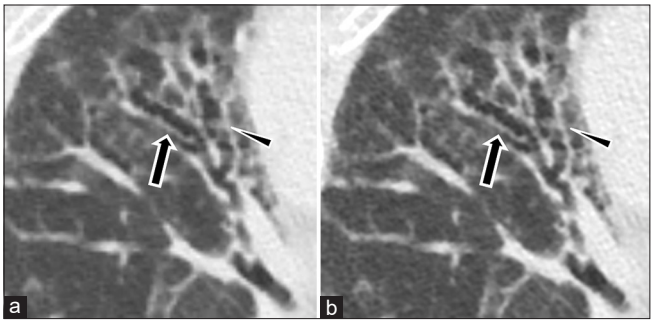

Figure 1: An 81-year-old female with idiopathic pulmonary fibrosis Compared to standard image reconstruction (a), high matrix image reconstruction, (b) is better in depicting thickened bronchial walls (black arrows) and an area of mucus plugging (arrowheads) in a right middle lobe bronchus. Relative conspicuity scores of 2 and 1 were rated by each reader.

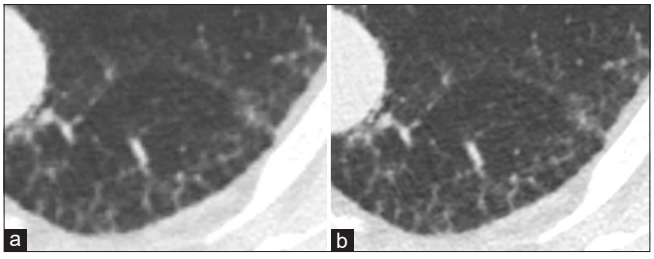

Figure 2: A 72-year-old male with idiopathic pulmonary fibrosis Compared to standard image reconstruction (a), intralobular reticular opacity in the peripheral lung is more distinct and better demonstrated in the left lower lung on high matrix image reconstruction (b). A relative conspicuity score of 2 was rated by both readers.

($P < 0.001$), but did not affect classification confidence for the other reader [Figure 6].

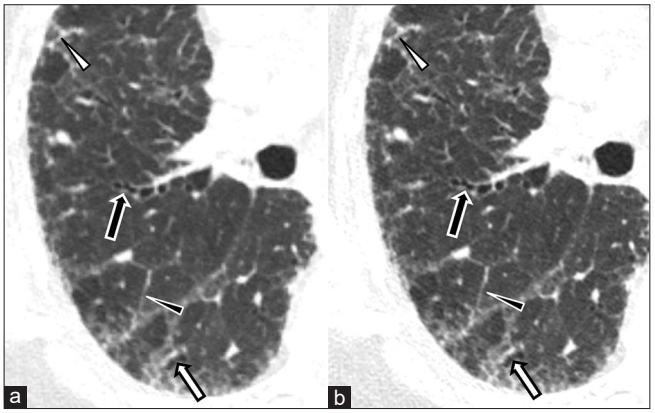

Figure 3: An 81-year-old female with idiopathic pulmonary fibrosis Compared to standard image reconstruction (a), traction bronchiectasis (black arrows), peripheral airway visualization (white arrows), interlobular septal thickening (black arrowheads), and intralobular reticular opacity (white arrowheads) are more clear on high matrix image reconstruction (b). Both readers rated these abnormalities as being present and high matrix image reconstruction demonstrating higher relative conspicuity scores for each of the above four imaging findings.

Image quality

Image quality scores were significantly higher with high matrix image reconstruction compared to standard image reconstruction for both readers (R1 - 2.03 ± 0.17 vs. 2.63 ± 0.49, $P < 0.001$; R2 - 2.03 ± 0.24 vs. 2.81 ± 0.40, $P < 0.001$). One reader rated subjective noise and artifact slightly but significantly better for high matrix reconstruction, while the other reader thought the opposite (R1 - 2.75 ± 0.44 vs. 2.79 ± 0.41, $P = 0.003$; R2 - 2.81 ± 0.50 vs. 2.72 ± 0.62, $P = 0.030$, [Figure 7]).

DISCUSSION

This study demonstrated that high matrix image reconstruction provides increased conspicuity of abnormal pulmonary imaging findings compared to standard image reconstruction for two thoracic radiologists. Findings seen with usual interstitial pneumonia (UIP) pattern such as interlobular septal thickening ($P \leq 0.001$), intralobular reticular opacity ($P < 0.001$), and end-stage fibrotic changes including traction bronchiectasis and honeycombing ($P < 0.001$) were observed more clearly in high matrix image reconstruction compared to standard image reconstruction by both readers. Conversely, there was not a consistent trend toward increasing confidence in the identification or classification of pulmonary nodules using high matrix reconstruction.

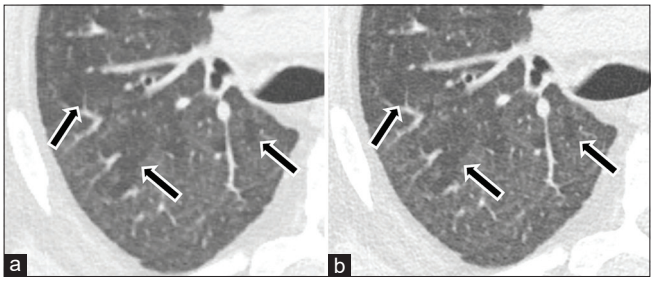

Figure 4: A 64-year-old man with chronic idiopathic bronchiolitis Compared to standard image reconstruction (a), the difference between low-attenuation pulmonary lobules (arrows) and surrounding high-attenuation lobules is more conspicuous in high matrix image reconstruction (b). Relative conspicuity scores of 1 and 2 were rated by each reader.

These results suggest high matrix image reconstruction can potentially contribute to improved diagnostic performance for diagnosing UIP pattern on CT images. For the treatment of idiopathic pulmonary fibrosis, early pharmacological management using antifibrotic agents such as nintedanib and pirfenidone can mitigate the decline in pulmonary

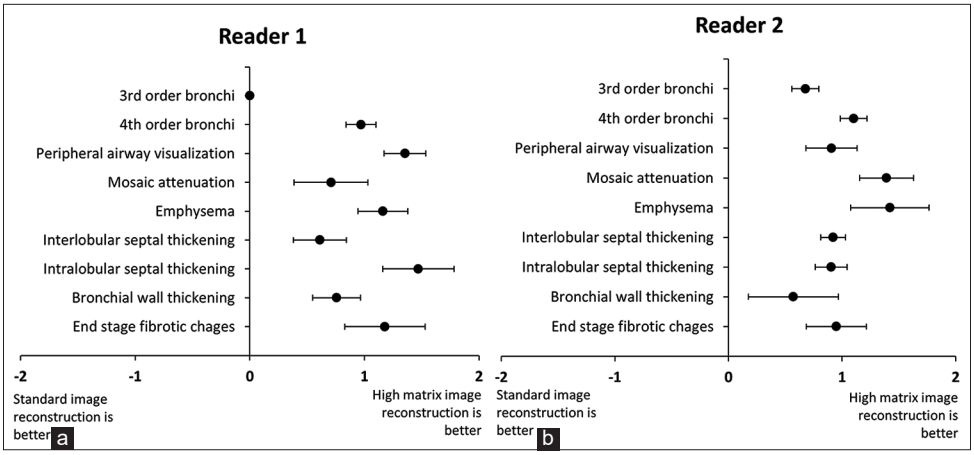

Figure 5: (a-b) Relative conspicuity scores of airway and parenchymal findings seen at high matrix image reconstruction are demonstrated in comparison to standard matrix by each of the two radiologist readers. Positive scores indicate that high matrix reconstruction better displayed the imaging finding (with zero representing equivalency). For each finding, the black dot represents the mean relative conspicuity score of the imaging finding on high matrix reconstruction compared to routine images with the bar representing the 95% confidence intervals. It can be seen that all findings for both readers were better visualized at high matrix reconstruction except 3rd order bronchi for one reader.

Table 4: Likelihood ratings for pulmonary nodule presence and confidence ratings for correct classification of internal attenuation characteristics.

	Reader 1			Reader 2		
	Standard image reconstruction	**High matrix image reconstruction**	***P*-value**	**Standard image reconstruction**	**High matrix image reconstruction**	***P*-value**
Likelihood						
Ground-glass	79.2±16.0	80.8±14.1	0.076	83.7±14.0	87.7±11.9	<0.001*
Part-solid	88.2±12.7	89.4±11.0	0.125	98.3±4.1	98.3±4.1	NA
Solid	94.2±9.0	94.2±9.5	1.000	99.5±2.1	99.7±1.7	1.000
Classification						
Ground-glass	74.8±12.3	83.2±9.4	<0.001*	98.5±4.9	98.5±4.9	NA
Part-solid	76.2±15.2	86.5±11.3	<0.001*	81.7±11.7	81.7±9.8	1.000
Solid	89.9±15.4	92.3±11.7	<0.001*	100±0	99.8±1.2	1.000

Wilcoxon-signed rank test, *:$P<0.05$

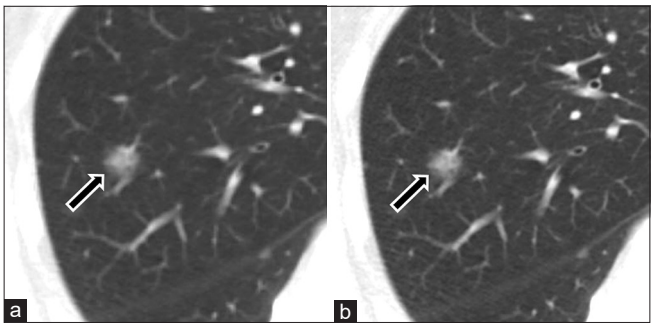

Figure 6: An 84-year-old woman presents with a part-solid nodule readers classified the nodule as part-solid and rated the likelihood score for nodule presence and confidence of internal attenuation classification as being similar at standard image reconstruction (a) and high matrix reconstruction (b).

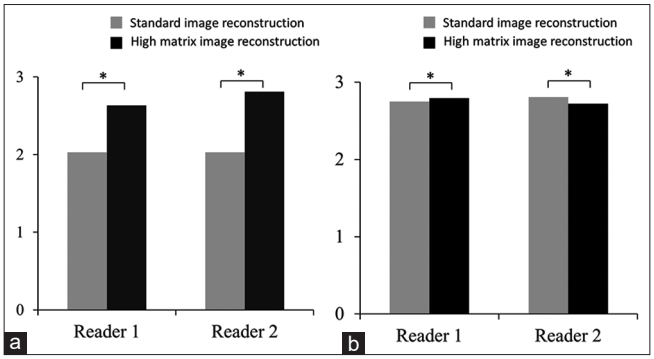

Figure 7: Result of overall image quality, subjective noise and image artifact. (a) Overall image quality: High matrix image reconstruction is significantly better than standard image reconstruction for both readers ($P < 0.001$). (b) Subjective image noise and artifact: High matrix image reconstruction varies slightly but significantly between the reconstructions for both readers. Wilcoxon-signed rank test.*$P < 0.05$.

function and improve the patient's prognosis,[12,13] but are expensive and can result in severe adverse events.[14] As such, multidisciplinary discussion involving clinicians, radiologists, and pathologists is important and widely accepted to insure the correct and reproducible diagnosis for idiopathic pulmonary fibrosis.[15] In patients who are clinically suspected of idiopathic pulmonary fibrosis, a surgical biopsy is not recommended for diagnosis when HRCT shows a typical UIP pattern of bilateral reticulation, traction bronchiectasis, and honeycombing distributed predominantly in the peripheral and lower lungs.[16] Given the findings in our study, high matrix image reconstruction may be of benefit in patients with known or suspected UIP. Readers demonstrated fair or moderate interobserver agreement ($\alpha = 0.335–0.466$) when evaluating these findings; not dissimilar to the previous studies with standard image reconstruction, typically showing moderate interobserver agreement in diagnosing UIP based on honeycombing, even by experienced thoracic radiologists.[17,18]

In contrast, several other chest CT findings such as upper-lung or peri-bronchovascular predominant fibrosis, significant parenchymal consolidation, and ground-glass opacity or mosaic attenuation are inconsistent with a UIP pattern and raise the possibility of an alternative interstitial lung disease.[19] High matrix image reconstruction did demonstrate mosaicism to a better extent than standard image reconstruction for both readers ($P \leq 0.001$). In terms of emphysema, high matrix image reconstruction was shown to better demonstrate areas of low attenuation in the lung parenchyma compared to standard image reconstruction ($P < 0.001$).

To increase CT image detail with smaller pixels, a smaller field of view with higher matrix is required. In the current study, we reconstructed CT images with a higher matrix (1024 × 1024) relative to standard image reconstruction (512 × 512). Pixel size is calculated by dividing field of view by matrix size; therefore, matrix parameters do influence pixel size; however, overall spatial resolution is determined by a combination of the detector element, reconstruction kernel, slice thickness, and CT system in addition to image matrix size.[10] In this study, estimated pixel sizes in all patients ranged from 0.664 to 0.898 mm for standard image reconstruction and 0.332–0.449 mm for high matrix image reconstruction [Table 2], both of which were larger than the 0.23 mm resolution reported in the Yanagawa *et al*. study using garnet based detectors.[20] In our study, pixel size is the limiting factor to the overall system's spatial resolution; therefore, it is expected that high matrix image reconstruction would demonstrate improved anatomic detail resulting in higher conspicuity and confidence levels in identifying some imaging findings by providing shaper CT images with less blurry borders.

Lung nodules are commonly identified on CT in routine clinical practice. These can be benign or malignant, with potential etiologies such as inflammatory processes, granulomas, atypical adenomatous hyperplasia, adenocarcinoma *in situ*, minimally invasive adenocarcinomas, invasive adenocarcinomas, and metastases which can be difficult to discriminate at a single time point.[7,21] Pulmonary nodule management is determined by the type of lung nodule (solid, part-solid, or ground-glass), its diameter on CT images, and patient risk factors.[22] High matrix image reconstruction improved confidence with regard to the presence and classification of internal attenuation for one reader only. Therefore, high matrix image reconstruction may not provide reliable improvement in pulmonary nodule detection and classification.

A previous study using the same CT platform as this study demonstrated that high matrix image reconstruction showed no significant difference in subjective evaluation of the

bronchial tree but higher image sharpness and image noise compared to standard image reconstruction[23] In studies investigating CT scanners utilizing a combination of smaller detector size (0.25 × 0.25 mm) and high matrix image reconstruction, the technique was beneficial in lung nodule evaluation,[24,25] peripheral airway assessment,[26] small pulmonary ossification detection,[27] quantitative emphysema measurement,[28] automatic bronchial segmentation,[29] and virtual bronchoscopy.[30] Although smaller detector size exploits the advantage of high matrix image reconstruction, it is uncertain how high matrix image reconstruction improves the performance of other diagnostic tasks when combined with conventional CT detector size.

There are some limitations to our pilot study. First, in the assessment of patients with more than four lung nodules, each reader-selected up to four lung nodules using a common prioritization scheme for nodule selection. As a result, paired comparison could not be performed, although the main purpose of this study was not to compare interobserver agreement but image construction technique. Second, high matrix image reconstruction requires longer reconstruction times and generates 4 times the data of standard image reconstruction and these disadvantages should be weighed when considering implementation of this technique. To view images, we enlarged routine images so that one lung filled each monitor. A practical method for viewing high matrix images in clinical practice will be important to take advantage of our findings; limiting the use of high matrix reconstruction to cases with known or suspected UIP may be one strategy. Third, we did not scan to determine spatial resolution using a slit phantom because our aim was to assess the clinical impact of high matrix image reconstruction in diagnosing pulmonary pathologies. Finally, high matrix image reconstruction may have different effects when combined with different scanning parameters such as reconstruction algorithm or radiation dose; however, in our study we sought to specifically compare 512- and 1024-matrices while fixing other parameters. As such, further studies could be beneficial in determining how modifying other scanning parameters might affect image quality in the setting of high matrix size.

CONCLUSION

High matrix image reconstruction can be of benefit to radiologists evaluating a wide range of chest pathology, particularly interstitial lung diseases by improving conspicuity of peripheral airway visualization, interlobular septal thickening, intralobular reticular opacity, and end-stage fibrotic change.

Acknowledgment

This research was presented and abstracted in Annual Meeting – Society of Thoracic Radiology in 2020.

Declaration of patient consent

The authors certify that they have obtained all appropriate patient consent.

Financial support and sponsorship

Nil.

Conflicts of interest

Cynthia H. McCollough – Grant to institution; Siemens Healthineers Joel G. Fletcher – Grant to institution; Siemens Healthineers No other authors have a conflict to disclose.

REFERENCES

1. Corcoran HL Renner RW, Milstein MJ. Review of high-resolution CT of the lung. Radiographics 1992;12:917-39.
2. Nishimura K, Kitaichi M, Izumi T, Nagai S, Kanaoka M, Itoh H. Usual interstitial pneumonia: Histologic correlation with high-resolution CT. Radiology 1992;182:337-42.
3. Murata K, Itoh H, Todo G, Kanaoka M, Noma S, Itoh T, *et al*. Centrilobular lesions of the lung: Demonstration by high-resolution CT and pathologic correlation. Radiology 1986;161:641-5.
4. Stein MG, Mayo J, Müller N, Aberle DR, Webb WR, Gamsu G. Pulmonary lymphangitic spread of carcinoma: Appearance on CT scans. Radiology 1987;162:371-5.
5. Zwirewich CV, Vedal S, Miller RR, Müller NL. Solitary pulmonary nodule: High-resolution CT and radiologic-pathologic correlation. Radiology 1991;179:469-76.
6. Almeida RF, Watte G, Marchiori E, Altmayer S, Pacini GS, Barros MC, *et al*. High resolution computed tomography patterns in interstitial lung disease (ILD): Prevalence and prognosis. J Bras Pneumol 2020;46:e20190153.
7. Lee JH, Park CM, Lee SM, Kim H, McAdams HP, Goo JM. Persistent pulmonary subsolid nodules with solid portions of 5 mm or smaller: Their natural course and predictors of interval growth. Eur Radiol 2016;26:1529-37.
8. Kakinuma R, Moriyama N, Muramatsu Y, Gomi S, Suzuki M, Nagasawa H, *et al*. Ultra-high-resolution computed tomography of the lung: Image quality of a prototype scanner. PLoS One 2015;10:e0137165.
9. Yanagawa M, Hata A, Honda O, Kikuchi N, Miyata T, Uranishi A, *et al*. Subjective and objective comparisons of image quality between ultra-high-resolution CT and conventional area detector CT in phantoms and cadaveric human lungs. Eur Radiol 2018;28:5060-8.
10. Hata A, Yanagawa M, Honda O, Kikuchi N, Miyata T, Tsukagoshi S, *et al*. Effect of matrix size on the image quality of ultra-high-resolution CT of the Lung. Acad Radiol 2018;25:869-76.
11. Bartlett DJ, Koo CW, Bartholmai BJ, Rajendran K, Weaver JM, Halaweish AF, *et al*. High-resolution chest computed tomography imaging of the lungs: Impact of 1024 matrix reconstruction and photon-counting detector computed tomography. Invest Radiol 2019;54:129-37.

12. Albera C, Costabel U, Fagan EA, Glassberg MK, Gorina E, Lancaster L, *et al*. Efficacy of pirfenidone in patients with idiopathic pulmonary fibrosis with more preserved lung function. Eur Respir J 2016;48:843-51.
13. Flaherty KR, Wells AU, Cottin V, Devaraj A, Walsh SL, Inoue Y, *et al*. Nintedanib in progressive fibrosing interstitial lung diseases. N Engl J Med 2019;381:1718-27.
14. Lederer DJ, Martinez FJ. Idiopathic pulmonary fibrosis. N Engl J Med 2018;378:1811-23.
15. Walsh SL, Wells AU, Desai SR, Poletti V, Piciucchi S, Dubini A, *et al*. Multicentre evaluation of multidisciplinary team meeting agreement on diagnosis in diffuse parenchymal lung disease: A case-cohort study. Lancet Respir Med 2016;4:557-65.
16. Raghu G, Remy-Jardin M, Myers JL, Richeldi L, Ryerson CJ, Lederer DJ, *et al*. Diagnosis of idiopathic pulmonary fibrosis. An official ATS/ERS/JRS/ALAT clinical practice guideline. Am J Respir Crit Care Med 2018;198:e44-68.
17. Watadani T, Sakai F, Johkoh T, Noma S, Akira M, Fujimoto K, *et al*. Interobserver variability in the CT assessment of honeycombing in the lungs. Radiology 2013;266:936-44.
18. Walsh SL, Calandriello L, Sverzellati N, Wells AU, Hansell DM, UIP Observer Consort. Interobserver agreement for the ATS/ERS/JRS/ALAT criteria for a UIP pattern on CT. Thorax 2016;71:45-51.
19. Lynch DA, Sverzellati N, Travis WD, Brown KK, Colby TV, Galvin JR, *et al*. Diagnostic criteria for idiopathic pulmonary fibrosis: A Fleischner society white paper. Lancet Respir Med 2018;6:138-53.
20. Yanagawa M, Tomiyama N, Honda O, Kikuyama A, Sumikawa H, Inoue A, *et al*. Multidetector CT of the lung: Image quality with garnet-based detectors. Radiology 2010;255:944-54.
21. Ko JP, Azour L. Management of incidental lung nodules. Semin Ultrasound CT MR 2018;39:249-59.
22. MacMahon H, Naidich DP, Goo JM, Lee KS, Leung AN, Mayo JR, *et al*. Guidelines for management of incidental pulmonary nodules detected on CT images: From the fleischner society 2017. Radiology 2017;284:228-43.
23. Euler A, Martini K, Baessler B, Eberhard M, Schoeck F, Alkadhi H, *et al*. 1024-pixel image matrix for chest CT-impact on image quality of bronchial structures in phantoms and patients. PLoS One 2020;15:e0234644.
24. Tsubamoto M, Hata A, Yanagawa M, Honda O, Miyata T, Yoshida Y, *et al*. Ultra high-resolution computed tomography with 1024-matrix: Comparison with 512-matrix for the evaluation of pulmonary nodules. Eur J Radiol 2020;128:109033.
25. Yoshida Y, Yanagawa M, Hata A, Sato Y, Tsubamoto M, Doi S, *et al*. Quantitative volumetry of ground-glass nodules on high-spatial-resolution CT with 0.25-mm section thickness and 1024 matrix: Phantom and clinical studies. Eur J Radiol Open 2021;8:100362.
26. Tanabe N, Shima H, Sato S, Oguma T, Kubo T, Kozawa S, *et al*. Direct evaluation of peripheral airways using ultra-high-resolution CT in chronic obstructive pulmonary disease. Eur J Radiol 2019;120:108687.
27. Hata A, Yanagawa M, Tsubamoto M, Doi S, Yoshida Y, Miyata T, *et al*. Detectability of pulmonary ossifications in fibrotic lung on ultra-high-resolution CT using 2048 matrix size and 0.25-mm slice thickness. Sci Rep 2021;11:15119.
28. Xu Y, Yamashiro T, Moriya H, Muramatsu S, Murayama S. Quantitative emphysema measurement on ultra-high-resolution CT scans. Int J Chron Obstruct Pulmon Dis 2019;14:2283-90.
29. Morita Y, Yamashiro T, Tsuchiya N, Tsubakimoto M, Murayama S. Automatic bronchial segmentation on ultra-HRCT scans: Advantage of the 1024-matrix size with 0.25-mm slice thickness reconstruction. Jpn J Radiol 2020;38:953-9.
30. Adachi T, Machida H, Nishikawa M, Arai T, Kariyasu T, Koyanagi M, *et al*. Improved delineation of CT virtual bronchoscopy by ultrahigh-resolution CT: Comparison among different reconstruction parameters. Jpn J Radiol 2020;38:884-9.

How to cite this article: Inoue A, Johnson TF, Voss BA, Lee YS, Leng S, Koo CW, *et al*. A pilot study to estimate the impact of high matrix image reconstruction on chest computed tomography. J Clin Imaging Sci 2021;11:52.